REPORT DOCUMENTATION PAGE	Form Approved OMB NO. 0704-0188

Public reporting burden for this collection of information is estimated to average 1 hour per response, including the time for reviewing instructions, searching existing data sources, gathering and maintaining the data needed, and completing and reviewing the collection of information. Send comment regarding this burden estimates or any other aspect of this collection of information, including suggestions for reducing this burden, to Washington Headquarters Services, Directorate for Information Operations and Reports, 1215 Jefferson Davis Highway, Suite 1204, Arlington, VA 22202-4302, and to the Office of Management and Budget, Paperwork Reduction Project (0704-0188), Washington, DC 20503.

1. AGENCY USE ONLY (Leave blank)	2. REPORT DATE December 1996	3. REPORT TYPE AND DATES COVERED Final Report: 1 Jul 92-31 Dec96

4. TITLE AND SUBTITLE	5. FUNDING NUMBERS
Atmospheric Turbulence Detection in Three Dimensions by Means of a Multiple Beam SODAR	DAAL03-92-G-0278

6. AUTHOR(S)

R.L.N. Mandock and J.D. Echard

7. PERFORMING ORGANIZATION NAMES(S) AND ADDRESS(ES)	8. PERFORMING ORGANIZATION REPORT NUMBER
Georgia Institute of Technology Atlanta, GA 30332	

9. SPONSORING / MONITORING AGENCY NAME(S) AND ADDRESS(ES)	10. SPONSORING / MONITORING AGENCY REPORT NUMBER
U.S. Army Research Office P.O. Box 12211 Research Triangle Park, NC 27709-2211	ARO 30476.1-GS

11. SUPPLEMENTARY NOTES

The views, opinions and/or findings contained in this report are those of the author(s) and should not be construed as an official Department of the Army position, policy or decision, unless so designated by other documentation.

12a. DISTRIBUTION / AVAILABILITY STATEMENT	12 b. DISTRIBUTION CODE
Approved for public release; distribution unlimited.	19970210 084

13. ABSTRACT (Maximum 200 words)

An acoustical remote sensor has been developed to image the three-dimensional structure of atmospheric turbulence in the atmospheric boundary layer. The system is designed to detect the evolution and decay of microscale turbulence structures, the motions of individual microscale eddies, and characteristics of the mean wind in the lower boundary layer. The methodology consists in illuminating roughly half a steradian of the boundary layer with a powerful acoustical interferometer antenna, recording the backscattered signal through multiple simultaneous beams, and analyzing the adquired data for turbulence intensity and Doppler wind velocity. A commercial (Remtech PA-3) sodar is available to serve as a standard against which to compare these measurements in the vertical beam.

14. SUBJECT TERMS		15. NUMBER IF PAGES 21
Atmospheric Turbulence, Detection, SODAR		16. PRICE CODE

17. SECURITY CLASSIFICATION OR REPORT	18. SECURITY CLASSIFICATION OF THIS PAGE	19. SECURITY CLASSIFICATION OF ABSTRACT	20. LIMITATION OF ABSTRACT
UNCLASSIFIED	UNCLASSIFIED	UNCLASSIFIED	UL

DTIC QUALITY INSPECTED 1

CONTENTS

FORWARD

This study was performed by the Georgia Tech Research Institute (GTRI) at the Georgia Institute of Technology (GIT), using U.S. Army Research Office (ARO) funds for FY92-96. The authors are indebted to Walter Flood and Walter Bach of ARO for their sponsorship and encouragement; to Robert W. McMillan of GTRI/USAF Rome Laboratory for service as first principal investigator, scientific advisor and trusted colleague throughout the study; to Gerald Grams and Steve Fischer of Clark Atlanta University for assistance in field work and software development; to Fr. Mark Fischer and Dennis Bouchard of St. Francis de Sales Latin Mass Community, Atlanta, for providing the experimental site location and technical support; to Robert G. Roper of the School of Earth and Atmospheric Sciences, GIT, for advising Mr. Mandock on aspects of the study pertinent to his doctoral dissertation; and to Wayne Cassaday of GTRI for serving as second principal investigator midway through the study.

LIST OF ILLUSTRATIONS AND TABLES

SECTION I. Statement of the Problem Studied

BACKGROUND

The statistical description of the atmospheric wind and temperature turbulence fields has proven useful to the understanding and prediction of turbulent transport and mixing of geophysical fluids based on small scale models in the laboratory. In situ and linear remote sensing measurements have provided substantial empirical information in the study of atmospheric turbulence, but these methods are somewhat dependent on assumptions such as stationarity and "frozen in" structures, which limit their predictive skill for the most part to the current state of the art. Although commercial and research determinations of the total wind vector by acoustical means make use of phased array antenna technology, these devices generally rely on linear beam paths along three independent axes that do not simultaneously sample the same turbulence backscattering volume in the atmospheric boundary layer. Averaging over an ensemble of sequential radar pulsings for 15-20 minutes is believed to overcome this difficulty by relying on assumptions such as those mentioned above. Useful as these analyses may be, they are nonetheless only modifications of the linear (pencil beam) remote sensing techniques of the past.

Given the present state of knowledge about the spatial structure and temporal variation of atmospheric surface layer turbulence for scale sizes near the low-wavenumber end of the equilibrium range, researchers at Georgia Tech have begun an effort to attempt to observe details of the evolution and decay of turbulence structures which persist in the wind field and are transported with the mean wind. In order for this variation in structure to be observed by a remote sensor, the physical dimension of the disturbance must be small enough to undergo marked change while passing through the illuminated volume of a wide-beam active device. The appropriate dimension is approximately the outer scale of turbulence near the ground. Measurements indicate that the outer scale (large-scale cutoff of the inertial subrange) lies between about 10 meters and a few tens of meters, depending on atmospheric stability (Brown and Hall, 1978). Tatarskii (1971) characterizes the outer scale in the surface layer as approximately 0.4z, where z is height above ground. The typical dimensions of dust devils and convective turbulence sheets transverse to the vertical beam of a sodar (sound detection

1

and ranging) device are on this order of meters.

Where the inertial subrange in the turbulence spectrum exists in the illuminated volume of a sodar, the eddies responsible for signal backscatter respond quickly to changing conditions in the mean flow and are thus in approximate equilibrium with local conditions in the mean flow (Tennekes and Lumley, 1972). The backscattering eddies become a form of tracer in this case. The pulse-by-pulse tracking of a coherent energy-bearing structure can be measured to provide a value for the mean wind, and inferences about larger scale eddy motions can be derived from pulse-by-pulse radial wind measurements.

An instrument capable of measuring wind and temperature fields rather than profiles should be able to determine the average properties of turbulent structures more efficiently than the sodars commercially available. For example, a volume-averaged surface kinematic heat flux and estimate of the eddy dissipation by means of transverse structure functions derived from a single transmit pulse is perhaps able to be measured by a wide beam sodar if the absolute transfer characteristics of the system are quantifiable. Another approach is to measure the relative magnitudes of temperature turbulence backscatter intensity and Doppler wind speed for individual volume grid locations within the field of view. This type of effort should be able to be used to map the inhomogeneity of turbulence and its variation with time in the lower atmospheric boundary layer.

THE INSTRUMENT

Recognizing the advantages that true three-dimensional imaging of the wind and temperature turbulence fields may allow, researchers at GTRI chose to attempt to develop an acoustical imaging remote sensor that would provide a three-dimensional grid of turbulence backscatter cells within an illuminated volume of about half a steradian solid angle. A broad-beam connected-interferometer (Green, 1985; Papas, 1988) transmitter has been constructed for this purpose from off-the-shelf components (a pair of Community M4 midrange compression drivers attached to PC1594M rectangular compound conical exponential horns). This acoustical antenna is designed to transmit a 2 kHz rectangular pulse into a conical region of the sky roughly 80 degrees by 70 degrees in angular extent. The receiver consists of 25

transducer elements in a square array of roughly 0.75-wavelength inter-element center spacing. Each receiver element is composed of a pair of Motorola KSN1025A piezo ceramic horn tweeter speakers which have been modified to fit into an array that is designed to allow for Dolph-Tschebyscheff amplitude tapering (Albers, 1965; Stutzman and Thiele, 1981).

The transmitter has been designed to generate a fan beam in the x-z plane and a tapered envelope that consists of a grating lobe on either side of the central lobe in the y-z plane. Figures 1 and 2 are models of the system's beam pattern in the y-z plane, based on calibration measurements provided by the manufacturers of the transmitting and receiving transducers and on a simulation program for an arbitrary array (Stutzman and Thiele, 1981). The 50 exponential-style horn loudspeakers of the receiver array are connected as pairs in series in order to increase their gain. The interference pattern resulting from this arrangement is shown by the simulation to not significantly degrade the antenna pattern of the array. Figures 3 and 4 illustrate the system's beam pattern in the x-z plane. Note that the receiver's antenna pattern is the dominant determinant of the system beam pattern in this plane, since the transmitter horns do not interfere along that surface.

Although Figure 5 suggests that the instrument is not technically a monostatic configuration, in essence it is so. The angular distance subtended by the greatest dimension across the sodar as observed at 100 meters in the far field is less than a degree. Because of this the primary backscatter mechanism is temperature turbulence, as seen in the expression below (Morris and Hall, 1975):

$$\sigma(\theta) = 0.055 \ \lambda^{-1/3} \cos^2 \theta \ \left[\frac{C_v^2}{c^2} \cos^2 \frac{\theta}{2} + 0.13 \ \frac{C_T^2}{T^2} \right] \left[\sin \frac{\theta}{2} \right]^{-11/3}$$

Here σ represents the acoustic backscatter cross section along a scattering angle from incidence θ, λ is the acoustic wavelength, C_v^2 and C_T^2 are the structure parameters of wind and temperature turbulence, and c is the speed of sound in air at temperature T. It is assumed that the sodar under study is effectively monostatic. Figure 6 is a system diagram of the

3

sodar.

For any monostatic sodar each backscatter element consists of a single fluctuation in acoustic refractivity proportional in size to the Bragg scattering distance $d = \pi/(k \sin \phi/2)$, where k is the acoustic wavenumber and ϕ is the scattering angle (Tatarskii, 1971). This scale size d is typically one-half the transmitted wavelength for a monostatic sodar, on the order of 9 cm for the 2-kHz device under study. Wavelets scattered from eddies which satisfy the Bragg condition produce a partially coherent scattered wave. Brown and Hall (1978) label this interaction a "coherent scattering process," and explain it as being due to the integrated effect of many small scatterings over a nonzero region of space. Turbulence is thus treated as a regular crystal lattice with lattice spacing d. As long as π/k is less than the outer scale, the random turbulence field can be decomposed by a spatial Fourier transform, and a Fourier component can be found that will satisfy the Bragg condition and produce coherent scattering.

METHODOLOGY

The methodology for the study consists in illuminating a broad conical sector of the atmospheric boundary layer with a powerful acoustical antenna and recording the backscattered signal through multiple simultaneous beams. The combination of interferometer transmitter and phased-array receiver results in predicted half-power beam widths of about 9 degrees in the y-z plane and about 15 degrees in the x-z plane. These Beamwidths as a function of height above ground level z for various look angles in Table 1. The width of the illuminated volume is given as a function of height for the x-z and y-z planes in Table 2. Each of the beams is additionally sectioned in the radial direction, thus producing a string of cylindrical cells. These cells are roughly 25 meters in length when the sodar is pulsed at its nominal operating duty burst of about 200 milliseconds.

A dissipation time scale may be estimated for eddies corresponding to the beam dimensions given in Table 1 by the inverse of the strain rate $1/s(k)$. In the inertial subrange of turbulence $s(k)$ is given by Tennekes and Lumley (1972) as

$$s(k) = \left[\frac{1}{2\pi}\right] \beta^{1/2} \epsilon^{1/3} k^{2/3}$$

This expression may be written as $0.133\,d^{-2/3}$, where β is a constant that is taken as 1.5, ϵ is the eddy dissipation, taken to be $0.005\ m^2\,s^{-3}$ (Robinson, 1984), and d is scale size. Thus, the time scales for the sodar under study range from about 2 seconds for the Bragg condition to as much as 10 minutes for the estimated maximum sodar range.

The echosonde equation (Brown and Hall, 1978) may be used to find the expected signal level for any range:

$$SPL_R = SPL_T + 10 \log(\tau A / 2) + 10 \log \sigma - 20 \log R - 2\alpha R$$

where SPL_R is the detected sound pressure level at a reference distance (taken as 1 meter here), SPL_T the transmitted sound pressure level, τ the transmitted pulse length, A an aspect factor to account for beam overlap (Pierce, 1981), and σ the total attenuation coefficient for air (Harris, 1966). From environmental noise measurements in rural Georgia, the estimated range calculates to be about 200 meters. This range calculation underestimates the maximum possible range because it allows a minimum signal to noise ratio of 13 dB and because it is based on detection by a single receiver element, the directive gain of the remaining 24 elements when phased and summed being ignored. Assuming this value as a conservative estimate of the typical range and given a transmit pulse duration of 0.2 seconds, about 5 levels of grid cells are expected in the radial direction. Given the 3 beams in the y direction imposed by the system design, the 5 levels in the z direction due to the Doppler pulse length and estimated system range, and arbitrarily choosing 7 beams in the x direction results in a total of 105 volume elements or grid cells in the illuminated region. For a 6 second pulse repetition rate, 100 realizations of this field can be recorded in a 10 minute data run. Table 2 indicates that this data acquisition protocol will permit 4 successive observations of a turbulence structure as it passes through the field of view at 200 meters height above ground.

The system parameters of bandwidth, carrier frequency and pulse length determine the maximum Doppler wind speed and minimum Doppler resolutions able to be measured. A bandwidth of 200 Hz has been chosen to limit the amount of environmental noise detected. Vertical wind fluctuations on the order of 1 m/s will permit maximum horizontal winds of 11 m/s to be detected by the beams of greatest steering angle. This value increases to 14 m/s for the next beam in (see Table 1, x-z plane), and beyond that for beams of lesser steering angle. The transmitted pulse length allows a minimum theoretical FFT resolution of about 0.43 m/s (4.88 Hz bin spacing) and a frequency error estimate (Levanon, 1988) of about 0.18 m/s in Doppler wind speed (assuming a signal to noise ratio of 2).

SUMMARY

An acoustical remote sensor has been developed to image the three-dimensional structure of atmospheric turbulence in the atmospheric boundary layer. The system is designed to detect the evolution and decay of microscale turbulence structures, the motions of individual microscale eddies, and characteristics of the mean wind in the lower boundary layer. The methodology for the study consists in illuminating roughly half a steradian of the boundary layer with a powerful acoustical interferometer antenna, recording the backscattered signal through multiple simultaneous beams, and analyzing the acquired data for turbulence intensity and Doppler wind velocity. A commercial sodar (Remtech PA-3) is available to serve as a standard against which to compare these measurements in the vertical beam.

SECTION II. Summary of the Most Important Results
STATUS OF THE STUDY

The study remains in progress at the time of this report. To date all electronic, mechanical and acoustical systems have been constructed and are functioning as designed. Three data runs have been made with the sodar, and preliminary analysis indicates that it is meeting its design specifications. The transmit transducers are capable of being driven in parallel without significant distortion by an amplifier generating greater than 550 watts output

power. This type of performance agrees with earlier test measurements of a single transducer. Each receiver channel is taking valid data, although drift appears to have changed their spectral responses slightly since their laboratory calibration about 6 weeks prior to the field data acquisition.

Data acquisition software performs as designed and operated well without incident. The analysis software written to date has proven useful for a quick look at the data, but is inadequate for purposes of intercomparison with the calibration standard device, a commercial Remtech PA-3 phased-array sodar. New software is currently being written and tested. This software is designed to analyze 312 megabytes (10 minutes) of data in terms of spectral and statistical analyses. Specific tasks underway include software to remove channel skew introduced by the multiplexing analog-to-digital (a/d) converters in each of the two data acquisition computers, software to stack individual FFT windows of 0.2048-second duration across all 25 receiver channels, software to stack all 25 received signal traces along the entire 10 minute data run (12 megabytes), software to perform simple statistical analysis on the FFT windows from transmit pulse to transmit pulse along an entire trace. This software should be operating as designed by the end of the year. Software which has just been written to locate the transmit pulses on the 25-channel data files and on the pulse recording channel 26, is being used to search for harmonic distortion in the transmit pulse and to compare its center frequency with the frequency recorded by an analog meter during the data acquisition runs.

The sodar was left on site because beam pattern measurements and receiver calibrator response tests have not yet been completed. These calibrations will supplement the simulation data on hand and the meteorological verification of the sodar's performance. The meteorological verification plan has been revised due to procurement of the Remtech PA-3 sodar. At the start of the study it was planned that meteorological verification would consist of photographing several levels of smoke trails which would be generated by a number of smoke candles suspended on a tether below a meteorological balloon. These were to be ignited according to instructions by Carmen Nappo at NOAA's Atmospheric Turbulence and Diffusion Laboratory in Oak Ridge. The photographic record of swirling smoke trails passing through the field of view while the sodar recorded data was to have provided visual

7

confirmation of the sodar's reliability. However, that plan was dropped when the PA-3 became available because of the design and capability of this device.

The Remtech PA-3 is provided by Gerald Grams of Clark Atlanta University, who is working with one of the authors to develop a mobile environmental research laboratory. The current capability of this laboratory is primarily the PA-3 sodar, but by March of next year it should be operating with a Nd:YAG lidar, an aerosol spectrometer and a 30-meter tower outfitted with a sonic anemometer and 5 levels of profile instruments. The particular value of the PA-3 as a verification standard for the sodar under study is primarily its design. It consists of a phased array of 432 Motorola transducers which use the same acoustical driver as the sodar under study. The operating characteristics such as primary carrier frequency, pulse duty cycle, and receiver time gate, are very near those of the sodar under study. The PA-3 outputs a listing which updates every 15 minutes and provides a measurement of the environmental background acoustic noise and a estimate of the mean wind speed, the vertical wind speed, the standard deviations of the three component wind speeds and wind direction, and C_T^2 for each receiver time gate. The time gates can be set to equal that of the sodar under study, 35 meters.

RESULTS TO DATE

Three data acquisition runs have been made, each providing 20 minutes of data. Just prior to sodar system turn on and immediately after stopping data acquisition, the PA-3 was turned on in order to record data which would document the mechanical and thermal state of the atmosphere and bracket the measurements of the sodar under study. After thirty minutes of PA-3 operation, this sodar was turned off so that the receiver transfer function calibration could be recorded before the sodar receivers would be subject to drift. Two calibration runs were made for each 20 minute run.

Figure 7 plots a time series of data from a single transmit pulse. Both plots are of the same time series and are subject to compression due to the inability of the printer to plot 30,000 data points on a single page. The plots are therefore undersampled as represented and reveal roughly one out of every 14 data points in the actual time series. Even so, the data

traces manifest structure. The upper plot is time aligned with the lower and merely expands the vertical axis. The beginning of the transmit pulse is evident on the lower plot. The pulse duration is about 0.2152 seconds. Where it ends is not readily apparent on most of the traces because of the strong received signal which immediately follows the transmit pulse. Insufficient analysis has been done to date that would allow a characterization of the large signal strength just after the end of the transmit pulse. It may represent ringing in the receiver acoustical enclosure; it may be reflection and scatter off surface objects nearby; it may be true turbulence backscatter, which is usually significant near the ground; or it may be a combination of these factors. Attenuation of the signal with increasing travel time due to spherical divergence of the wavefront may be perceived in certain of the recorded signatures. It should be pointed out that the transmit pulse portion of the data does not completely represent the actual pulse detected by the receivers, but a voltage which is clipped by the protection diodes at the input of the receiver preamplifiers. The pulsed waveform which was sent to the transmitter was recorded on a separate channel for analysis and timing purposes.

CONCLUSIONS

The sodar under study by all indications is operating properly. All receiver channels, the transmitter, the calibrators and the data acquisition software are performing as expected. Backscattered signal has been detected from heights above ground of 260 to 330 meters.

Analysis of the acquired data is still in progress, but preliminary results indicate that the sodar may exceed the conservative design predictions made on the basis of theoretical and simulation considerations.

RECOMMENDATIONS

As the analysis of the data runs is still in progress, the conclusion of the study will not be complete until Mr. Mandock finishes his doctoral dissertation. This is expected to occur in March 1997. On completion, Mr. Mandock will forward copies of the thesis to ARO.

Possible ringing in the received signals just after transmit pulsing may be accentuated by the square walls of the four-sided wood and foam acoustical shield that surrounds the receiver

array. A fifth wall has been constructed so that the shield may be modified to a pentagonal design. Tests should be run to determine whether adding a fifth wall of the enclosure.

The sodar is a research instrument, and as such it requires substantial setup time. It is also susceptible to environmental noise, producing a downgraded signal in noisy environments. A more permanent site at a rural location would be a better solution than the suburban site currently chosen.

A closer look should be given to making the system more portable, given that it was not designed for extensive deployment in a rainy climate.

SECTION III. List of Publications and Technical Reports

No publications or technical papers were published during the contract period.

SECTION IV. List of All Participating Scientific Personnel Employed on the Project

Randal L. N. Mandock, Graduate Research Assistant

James D. Echard, Principal Research Engineer

Robert W. McMillan, Principal Research Scientist

Wayne L. Cassaday, Senior Research Engineer

Nile F. Hartman, Principal Research Scientist

Michael L. Blyler, Systems Analyst I

SECTION V. Report of Inventions

No inventions were patented during the contract period.

SECTION VI. Bibliography

Albers, V. M. Underwater Acoustics Handbook - II. Penn State Univ. Press, PA, 1965, pp. 188-205.

Brown, E. H., and F. F. Hall, 1978: Advances in atmospheric acoustics. Rev. Geophys. Space Phys., 16, 47-110.

Green, R. M. Spherical Astronomy. Cambridge University Press, Cambridge, 1985, pp. 366-368.

Harris, C. M., 1966: Absorption of sound in air versus humidity and temperature. J. Acoust. Soc. Amer., 40, 148-159.

Levanon, N. Radar Principles. Wiley, New York, 1988, pp. 170-174.

Morris, A. L., and F. F. Hall, Jr., 1975: Remote sensing of the atmosphere by sound, Atmos. Technol., 6, 84-93.

Papas, C. H. Theory of Electromagnetic Wave Propagation. Dover Press, New York, 1988, pp. 151-153.

Pierce, A. D. Acoustics: An Introduction to Its Physical Principles and Applications. McGraw-Hill, New York, 1981, pp. 448-450.

Robinson, G. S. Atmospheric Characteristics Inferred from Acoustic Radar Data. Ph.D. thesis, University of Melbourne, 1984, pp. 197-199.

Stutzman, W. L., and G. A. Thiele. Antenna Theory and Design. John Wiley & Sons, New York, pp. 145-154.

Tatarskii, V. I. The Effects of the Turbulent Atmosphere on Wave Propagation. Nauka, Moscow, 1967. Israel Program for Scientific Translations, U.S. Dept. of Commerce, 1971, pp. 54, 81, 86, 97, 115, 160, 161, 217, 240. [NTIS No. TT 68-50464].

Tennekes, H., and J. L. Lumley. A First Course in Turbulence. MIT Press, Cambridge, Mass., 1972, pp. 254, 262-267, 282-283.

TABLE 1. SODAR BEAMWIDTHS

x-z look angle (degrees)	x-z beamwidth (degrees)	linear x-z beamwidth (meters)				
		z(m) = 30	50	100	150	200
0	13.5	7	12	24	36	47
10	14	8	12	25	37	50
18	13.5	8	12	25	37	50
24	14.5	8	14	28	42	56
28	15	9	15	30	45	60
33	15	9	16	31	47	63

y-z look angle (degrees)	y-z beamwidth (degrees)	linear y-z beamwidth(meters)				
0	8	4	7	14	21	28
16	8.5	5	8	15	23	31

TABLE 2. WIDTH OF ILLUMINATED VOLUME

z (m)	width in the x direction (m)	width in y direction (m)
30	40	17
50	65	30
100	130	60
150	200	90
200	260	115

12
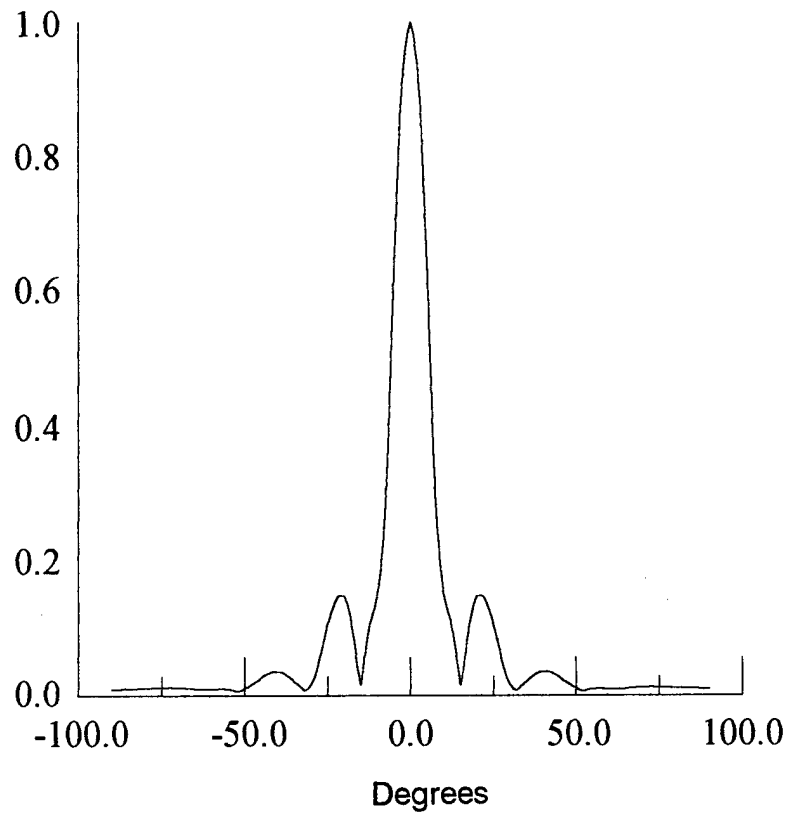
Figure 1. Rectangular plot of sodar antenna pattern in y-z plane.

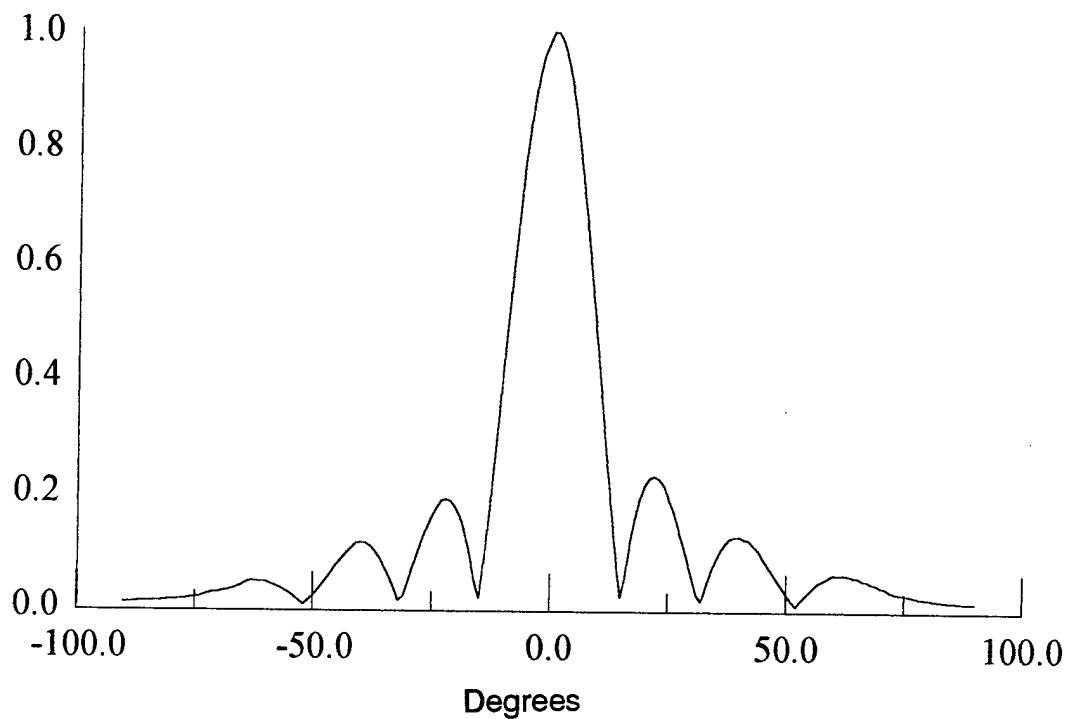Figure 2. Polar plot of sodar antenna pattern in y-z plane.

13

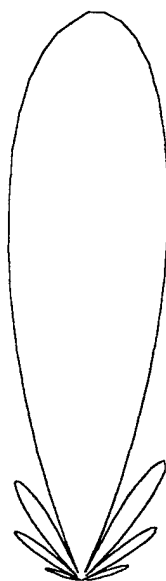Figure 3. Rectangular plot of sodar antenna pattern in x-z plane.

Figure 4. Polar plot of sodar antenna pattern in x-z plane.
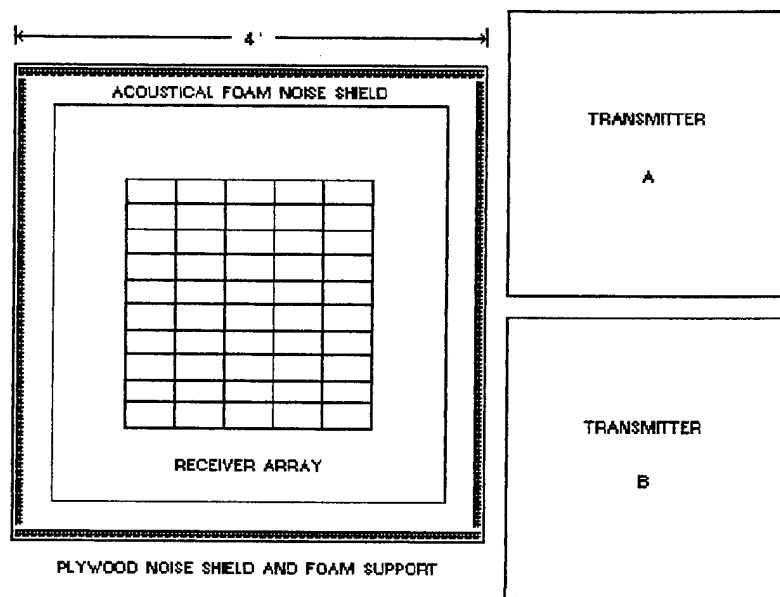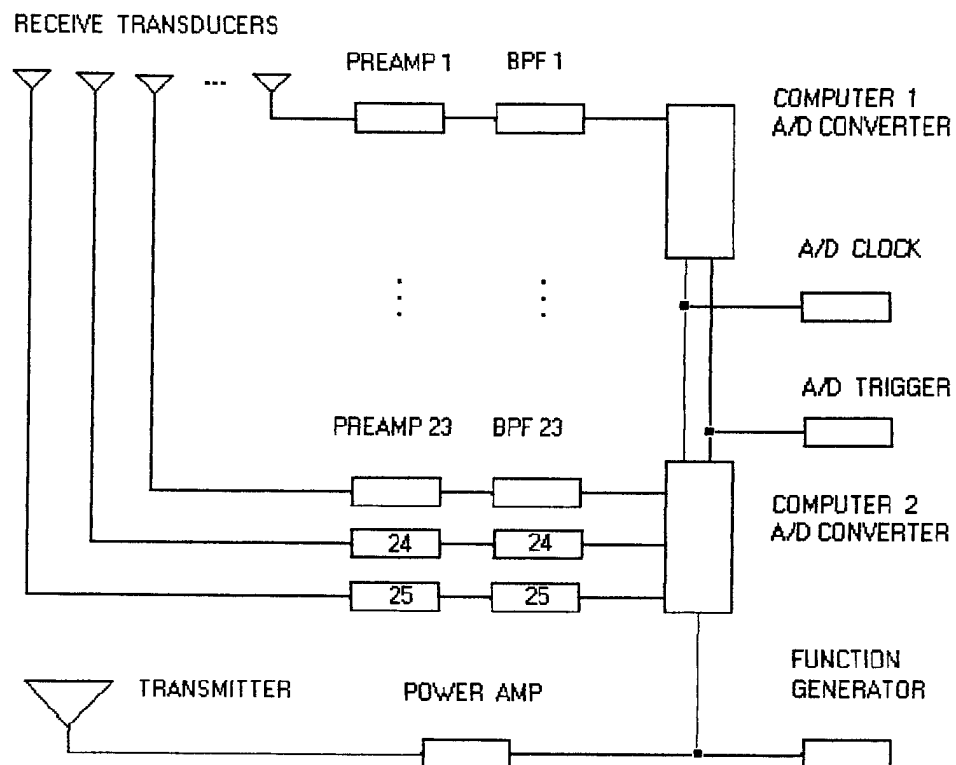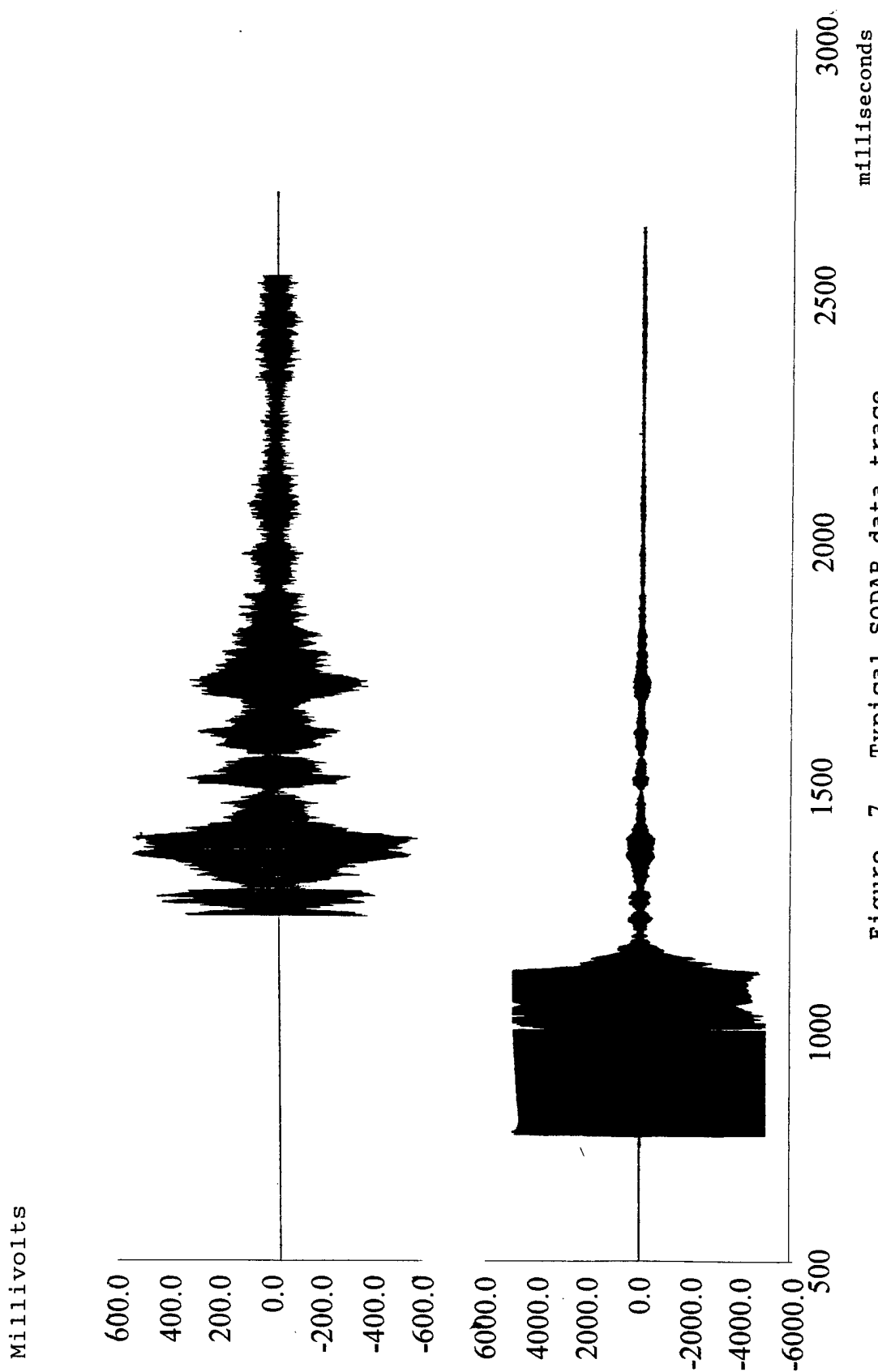
14

Figure 5. Plan view of sodar layout.

Figure 6. Sodar system diagram.

Figure 7. Typical SODAR data trace.